HAL open science

A simple analytical model for burr type prediction in drilling of ductile materials

Stéphane Segonds, Jacques Masounave, Victor Songmene, Christian Bes

To cite this version:

Stéphane Segonds, Jacques Masounave, Victor Songmene, Christian Bes. A simple analytical model for burr type prediction in drilling of ductile materials. Journal of Materials Processing Technology, 2013, 213 (6), pp.971-977. 10.1016/j.jmatprotec.2012.11.030 . hal-03832290

HAL Id: hal-03832290

https://hal.science/hal-03832290v1

Submitted on 27 Oct 2022

HAL is a multi-disciplinary open access archive for the deposit and dissemination of scientific research documents, whether they are published or not. The documents may come from teaching and research institutions in France or abroad, or from public or private research centers.

L'archive ouverte pluridisciplinaire **HAL**, est destinée au dépôt et à la diffusion de documents scientifiques de niveau recherche, publiés ou non, émanant des établissements d'enseignement et de recherche français ou étrangers, des laboratoires publics ou privés.

A simple analytical model for burr type prediction in drilling of ductile materials

Stéphane Segonds[a,*], Jacques Masounave[b,1], Victor Songmene[b], Christian Bès[a]

[a] Institut Clément Ader of Université Paul Sabatier, Toulouse, France
[b] LIPPS of Ecole de Technologies Supérieures, Montréal, Canada

ARTICLE INFO

Article history:
Received 20 September 2012
Accepted 27 November 2012
Available online 13 December 2012

Keywords:
Burr type
Prediction
Analytical model
Drilling

ABSTRACT

This paper proposes a new analytical model to predict the type of burr at drilling exit. The model is based on the theory of slip-planes and is specially developed to predict burr type formation in drilling of ductile materials. First the analytical model is set up, based on mechanical and geometrical considerations. Then it has been validated through experimental drilling tests on aeronautical aluminum by predicting burr type and thickness. The experimental results show that the model is suitable in the drilling of ductile materials and its validity domain has been established.

1. Introduction

Burr apparition at the exit of drilled holes significantly affects productivity since it makes deburring a necessary operation. Gillespie (1975) found that burr elimination may induce a 30% cost overrun and may often be manually done. In order to limit or suppress deburring operation, burr size must be decreased as possible. The modes of burr formation in exit of drilling as well as the influential parameters have already been studied through empirical methods, based on experimental observations. Nakayama and Arai (1987) give qualitative information on how to reduce burr size, on cutting angles and cutting condition and Lauderbaugh (2009) detail the burr formation stage and give indications on the influence of cutting angles on final bur height. These papers do not directly deal with the specific problem of drilling. A semi-analytical model is presented by Lauderbaugh (2009) by dividing a 3.175 mm drill cutting edge in 50 segments in order to determine the position of the segment at burr cap removal. This quite complex study has been validated on one specific drill geometry. The finite element method has been applied to the modeling of burr formation phenomenon by Klocke et al. (2004), Lauderbaugh and Saunders (2003) and Toropov and Ko (2006) studied and modeled burr formation, especially in feed direction. All the difficulties in a finite elements approach is to define realistic contact tool/part conditions and material behavior while cutting. However, burr formation in drilling process has not been described from an easy-to-use analytical point of view. So this study presents a model of exit burr formation in drilling of ductile materials based on the slip planes theory and a threshold to predict type B or C of burr formation is set up.

2. Burr formation model

2.1. Context

Burr is usually described by its height and its thickness, tagged as h_0 and b_g, for example by Heisel et al. (2005) and Schafer (1978). Schafer (1978) also detail other geometrical parameters that may be necessary to characterize more precisely the burr geometry, see for example r_f and b_f in their work. Others completing geometrical measurable parameters, burr shape (with or without cap, flash, etc.) can be examined to qualify burr from a morphological point of view. The present study focuses on the parameters that are burr type and burr thickness. Ko and Lee (2001) detail a burr type classification that is used along this paper:

Type A: no or very small burr.
Type B: burr with cap burr.
Type C: burr with burn-off marks.

Ko and Lee (2001) studied formation of different types of burrs, and geometry of the drill has been shown to have an important role on formation of type A, B or C burr. It has also been put in light that type B or C formation should be avoided since they are the most

* Corresponding author at: Université Paul Sabatier, Institut Clément Ader – 118 route de Narbonne, 31062 Toulouse Cedex 9, France. Tel.: +33 5 6155 7317; fax: +33 5 6155 8429.
E-mail address: stephane.segonds@univ-tlse3.fr (S. Segonds).

[1] Ecole de Technologie Supérieure, Laboratoire Ingénierie des Produits Procédés et Systèmes, 1100, rue Notre-Dame Ouest, Montréal (Québec) H3C 1K3, Canada.

0924-0136/$ – see front matter
http://dx.doi.org/10.1016/j.jmatprotec.2012.11.030

Nomenclature

f	feed rate (mm/rad)
R	drill radius (mm)
$R1$	drill radius for pre drilling (mm)
b	height before complete exit drill (mm)
bcrit	critical value of height (mm)
φ	complementary drill point angle (°)
Φ	shear angle (°)
Φ'	projection of Φ in M–M section (°)
α	rake angle (°)
λ	normal clearance angle (°)
θi	$i \in [1,6]$ angle between Si and Z axis (°)
$\theta\sigma$	angle between compression load direction and Z axis (°)
$\theta\tau$	angle between shear load direction and Z axis (°)
Si	$i \in [1,6]$ surface i of the sheared volume (mm^2)
Fz	cutting force along Z direction (N)
σy	part material yield strength (MPa)
σ	normal stress on S1 (MPa)
τ	shear stress on S1 (MPa)
κ	part material plasticity constraint (MPa)

difficult types of burrs to remove. So the present study focuses more precisely on prediction of type B or C of burr apparition. A threshold allowing to know if type B or C will be produced is setup knowing the machining context: drill geometry, machining conditions and part material.

2.2. Modelisation

Drill is assumed to be perfectly sharp and rigid and the study is relative to ductile material meaning that burr formation is without fracture.

As the drill moves toward the part, the distance between the cutting edge and the exit surface decreases. Obviously, there is a critical distance noted bcrit, under which cutting is not possible. The value of bcrit corresponds to the value of b (see Fig. 1) for which cutting forces induce a plastic deformation of the part remaining to be drilled: rigidity of the part to be drilled is not high enough to support cutting force. To determine this distance, the drilling studied configuration is presented in Fig. 1, illustrating different angles and quantities used along the paper.

Due to geometrical considerations, relation between Φ and Φ' is presented in Eq. (1). The shear angle Φ can be determined by Eq. (2), established by Lee and Shaffer (1951).

$$\frac{\tan(\Phi)}{\tan(\Phi')} = \cos(\phi) \tag{1}$$

$$\Phi = 45 + \alpha - \lambda \tag{2}$$

Toropov et al. (2005) and Toropov and Ko (2006) conducted experimental and analytical studies that have shown that burr formation in feed direction is caused by the stresses in the shear plane. The shear and normal stresses are considered uniform in the shear plane S1 (see Fig. 2). The cutting edge is represented by BF line and the rake and clearance angles are also considered as constants along BF line.

Since the exit surface is free from external stresses, the slip planes are inclined to the exit surface at 45° according to the theory of plasticity developed in Kachanov (1969) and Khan et al., 2008. Slip surfaces S2 to S6 are the boundaries of the tensile area. The sheared studied volume is presented in Fig. 2.

Surface ABFE is named S1, it corresponds to the sheared surface due to the drilling cutting forces. Surface ABGCDH

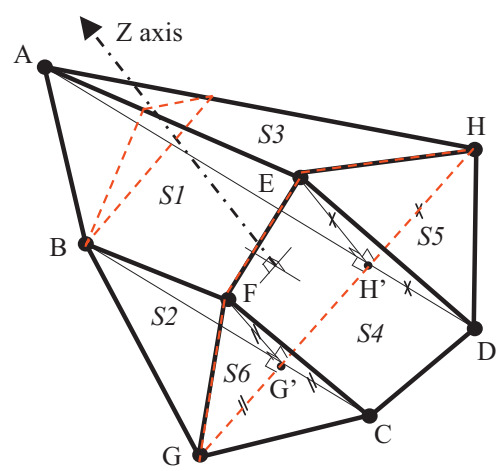

Fig. 2. 3D scheme of the sheared volume.

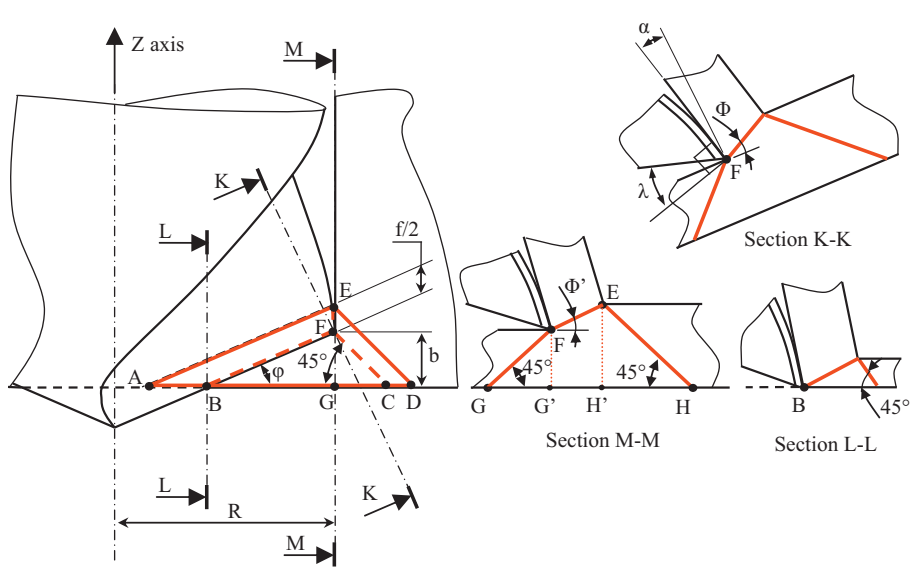

Fig. 1. Scheme for burr thickness determination.

corresponds to the surface where the drill exits. Due to geometrical properties of the studied configuration G′F = G′G = G′C = b and H′E = H′H = H′D = $b + f/2$.

Then equations of surfaces S1 to S6 are determined from geometrical properties of Figs. 1 and 2 as presented in Eq. (3):

$$S1 = \frac{f}{2 * \sin(\Phi')} * \left(\frac{b}{\sin(\varphi)} + \frac{f}{4 * \tan(\varphi)}\right) \tag{3.1}$$

$$S2 = \frac{b^2}{\sqrt{2}} * \sqrt{\left(\frac{1}{\tan(\varphi)}\right)^2 + \frac{1}{2}} \tag{3.2}$$

$$S3 = \frac{(b + (f/2))}{\sqrt{2}} * \sqrt{\left(\frac{2 * b + f}{2 * \tan(\varphi)}\right)^2 + \left(\frac{(b + (f/2))}{\sqrt{2}}\right)^2} \tag{3.3}$$

$$S4 = \left(2 * b - \frac{f}{2}\right) * \frac{f}{2\sqrt{2} * \tan(\Phi')} \tag{3.4}$$

$$S5 = \frac{\sqrt{3}}{2} * \left(b + \frac{f}{2}\right)^2 \tag{3.5}$$

$$S6 = \frac{\sqrt{3} * b^2}{2} \tag{3.6}$$

Angles θi between the normal to the surface Si and Z axis (see Figs. 1 and 2) can also be geometrically determined. Knowing that all the angles θi are in a range from 0° to 90°, they can be determined by the following equations:

$$\tan(\theta 1) = \frac{\tan(\varphi)}{\cos(\alpha)} \tag{4.1}$$

$$\tan(\theta 2) = \frac{1}{\cos(\varphi)} \tag{4.2}$$

$$\tan(\theta 3) = \frac{1}{\cos(\varphi)} \tag{4.3}$$

$$\tan(\theta 4) = \frac{1}{\cos(\Phi')} \tag{4.4}$$

$$\tan(\theta 5) = \sqrt{2} \tag{4.5}$$

$$\tan(\theta 6) = \sqrt{2} \tag{4.6}$$

2.3. Model for burr thickness prediction

2.3.1. Mechanical model

Loading on the studied volume presented in Figs. 1 and 4 is due to the cutting phenomenon and can been decomposed in a normal stress σ and a shear one τ, applied on surface S1 (see Fig. 3).

Since normal stress is directed on the normal to S1, then angle $\theta\sigma$ between normal stress direction on S1 and Z axis is $\theta\sigma = \theta 1$. Shear stress is directed perpendicularly to the cutting edge, so to BF line (see Fig. 1) in S1 and BF is along the radius of the hole, then angle $\theta\tau$ between shear direction and Z axis is $\theta\tau = 90 - \Phi'$.

The exit surface is free from external stresses and tension is expected in surfaces S2 to S6 due to the stresses applied on S1. When bcrit value is attained normal and shear stresses in S2 to S6 are equal to the value of plasticity κ, see Fig. 3. Shear stress is directed perpendicularly to the normal stress and in a plane that is perpendicular to Z direction. Value of plasticity κ is determined from σy, yield strength of workpiece material, according to the Mises criterion as $\kappa = (\sigma y)/\sqrt{3}$.

Then, equation of the force balance of sheared volume presented in Fig. 3 with respect to the Z-axis can be written as:

$$\kappa * ((\sin(\theta 2) + \cos(\theta 2)) * S2 + (\sin(\theta 3) + \cos(\theta 3)) * S3 + ((\sin(\theta 4) + \cos(\theta 4)) * S4 + (\sin(\theta 5) + \cos(\theta 5)) * S5 + (\sin(\theta 6) + \cos(\theta 6)) * S6 = (\sigma * \cos(\theta\sigma) - \tau * \cos(\theta\tau)) * S1 \tag{5}$$

For a given drilling configuration including tool geometry and part material characteristics, solving this equation conduces to determine the limit distance bcrit.

When the drill attains bcrit value, the cutting forces that are necessary to cut the material become too high in regard of the subsisting material rigidity. Then cutting forces cause plastic deformation of the workpiece material which is transformed into burr.

Initial height of studied volume (H′E distance, see Fig. 2) becomes the burr thickness after deformation and the value of bcrit corresponds to the value of the burr thickness.

2.3.2. Loads determination

For solving the previous equation of force balance, it is preliminarily needed to evaluate σ and τ for the studied drilling configuration. These two parameters are evaluated by force measurement during drilling. A predrilled hole (radius $R1$) is used in order to eliminate forces effect due to the drill web. Fz corresponds to the cutting force along Z direction, and the sheared area while drilling and before any point of the drill attaining the exit surface is noted S10. The relations between Fz, σ and τ coming from force balance with respect to Z axis are:

$$(\sigma * \cos(\theta\sigma) - \tau * \cos(\theta\tau)) * S10 = \frac{Fz}{2} \tag{6}$$

$$S10 = \frac{R - R1}{2 * \cos(\varphi) * \sin(\Phi')} \tag{7}$$

Combining the previous Eqs. (5)–(7) conduces to the expression of an equation combining geometrical drill parameters, b parameter and feed force as follows:

$$\kappa * ((\sin(\theta 2) + \cos(\theta 2)) * S2 + (\sin(\theta 3) + \cos(\theta 3)) * S3 + (\sin(\theta 4) + \cos(\theta 4)) * S4 + (\sin(\theta 5) + \cos(\theta 5)) * S5 + (\sin(\theta 6) + \cos(\theta 6)) * S6) = \frac{Fz * S1 * (R - R1)}{4 * \cos(\varphi) * \sin(\Phi')} \tag{8}$$

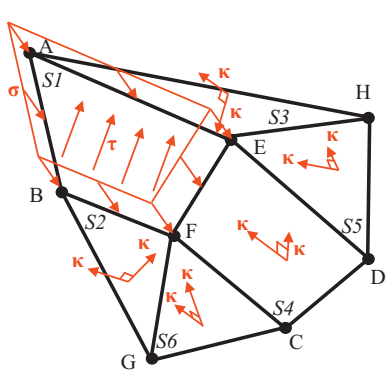

Fig. 3. Loadings on the studied sheared volume.

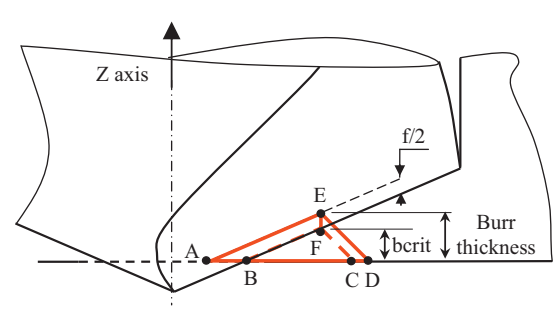

Fig. 4. Sheared volume scheme.

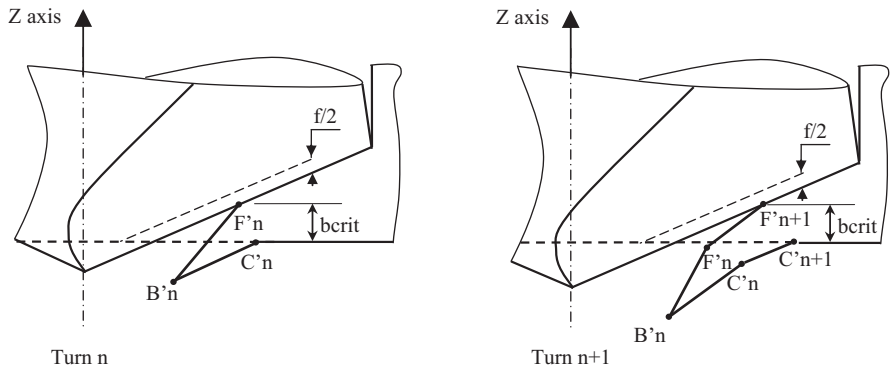

Fig. 5. Burr formation at drill exit between turn n and $n+1$.

In the following part, solution existence for this equation and its effect on bur type is discussed.

2.4. Burr type prediction

The previous part of the study proposes a model allowing determining a critical thickness value under which material part would plastically deform rather than supporting the cutting force. Many works on burr formation put in light the existence of three different types of burr. The further section details conditions of appearance of different burr types.

2.4.1. Burr type A

If Eq. (8) has no solution, it means that as thick as may be the rest of the part under the drill, and it is rigid enough to support the cutting force without any plastic deformation. In this case a type A of burr is obtained. Drill cutting edge totally exits the part and it is the secondary cutting edge, at the end of the drill margin, which cuts for the very end of the drilling. Results may differ from a test to another because of drill margin design that is varying between drill manufacturers. Nevertheless, cutting forces become tangential instead of being axial while cutting with main cutting edge, so burr generated in the last turn should be small and rake angle dependant. In this condition cutting force do not tend to make bending the rest of the part to be drilled. These considerations explain the fact that this configuration conduces to a type A of burrs, which is the case that requires the least removal cost.

2.4.2. Burr type B

If a bcrit value exists, it means that Eq. (8) has a solution, burr thickness may be modelized, and this thickness is equal to bcrit + $f/2$. Taking in account geometrical considerations, this section provides a modelization of burr type and burr height depending on feed rate. Indeed, the feed rate factor seems to have a high impact on burr type and on burr height as detailed by Lauderbaugh (2009) and Toropov and Ko (2006).

The reasoning detailed in the previous section may be applied at any moment of the drilling since the drill web has already went out of the part, like presented in Fig. 4.

Then, at any moment of the drill exit, there is a portion of the part remaining under the drill that is not rigid enough to support the cutting force without bending. This part corresponds to the volume studied in the previous section with a height that is equal to bcrit + $f/2$, see Fig. 4.

Existence of a bcrit value solution of Eq. (8) implies that half of the feed rate (feed rate/tooth) is smaller than burr thickness and burr formation can be explained as shown in Fig. 5.

When half of the feed rate is lower than burr thickness value, the burr grows at each turn of the drill because cutting edge cannot pass under the previously created burr. This explains that in these cutting conditions, a type B or C of burr is obtained. If drill web pierces the material while exiting the part that conduces to a type C of burr, in the other case it conduces to a type B.

These conditions, modelizing cutting of the burr at turn n + 1 while it has been initiated at turn n is quite difficult. But the proposed model evaluates burr type and thickness knowing machining conditions. From an industrial point of view that is an important information since burr type B or C must be avoided as possible, due to the high cost generated by their elimination with deburring operation.

Table 1
Drill geometry.

Drill	Diameter	Rake angle	Point angle
No. 1	8 mm	10°	135°
No. 2	8 mm	30°	135°
No. 3	8 mm	40°	135°
No. 4	8 mm	30°	115°
No. 5	12 mm	30°	135°

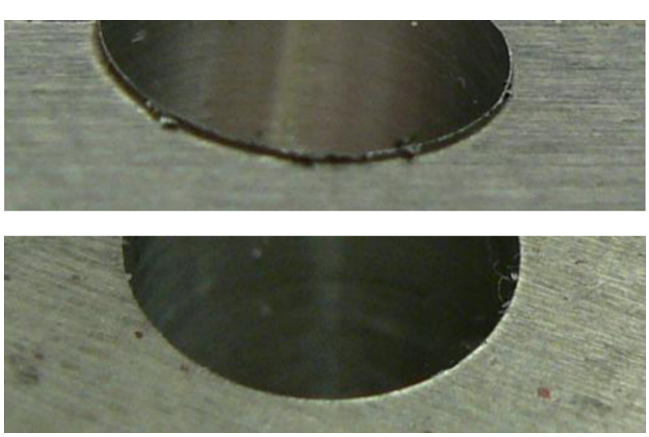

Fig. 6. (a) Detail of hole' edge (drill no. 3: 0.0125 mm/tr – 60 m/min). (b) Detail of hole' edge (drill no. 3: 0.025 mm/tr – 60 m/min).

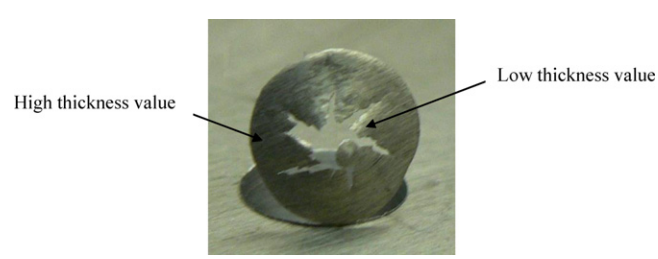

Fig. 7. Location of high and low values of thickness measurement.

Table 2
Experimental and theoretical results with drill nos. 1–5.

Drill no. 1				
Feed rate (mm/tr)	0.0125	0.025	0.05	0.1
Fz (N)	50	55	65	110
Predicted				
Burr type	Type B or C	Type B or C	Type A	Type A
bcrit value	0.016	0.011	–	–
Burr thickness	0.022	0.023		
Observation			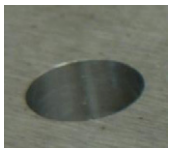	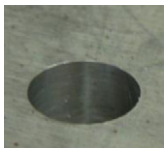
Measured				
Burr type	Type C2	Type B	Type A	Type A
Burr thickness	0.025	0.029–0.08	–	–

Drill no. 2				
Feed rate (mm/tr)	0.0125	0.025	0.05	0.1
Fz (N)	44	50	57	64
Predicted				
Burr type	Type B or C	Type B or C	Type A	Type A
bcrit value	0.013	0.008	–	–
Burr thickness	0.019	0.021		
Observation			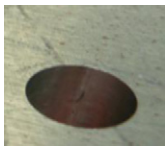	
Measured				
Burr type	Type B	Type B	Type A	Type A
Burr thickness	0.022–0.07	0.030–0.08	–	–

Drill no. 3				
Feed rate (mm/tr)	0.0125	0.025	0.05	0.1
Fz (N)	24	30	37	45
Predicted				
Burr type	Type B or C	Type A	Type A	Type A
bcrit value	0.003	–	–	–
Burr thickness	0.009			
Observation			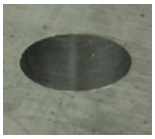	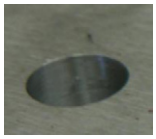
Measured				
Burr type	Type A	Type A	Type A	Type A
Burr thickness	–	–	–	–

Drill no. 4				
Feed rate (mm/tr)	0.0125	0.025	0.05	0.1
Fz (N)	20	69	84	95
Predicted				
Burr type	Type B or C	Type B or C	Type B or C	Type A
bcrit value	0.013	0.010	0.003	-
Burr thickness	0.019	0.023	0.028	
Observation				

Table 2 (*Continued*)

Drill no. 4				
Feed rate (mm/tr)	0.0125	0.025	0.05	0.1
Fz (N)	20	69	84	95
Measured				
Burr type	Type C2	Type C2	Type C2	Type A
Burr thickness	0.025	0.030	0.030	–

Drill no. 5				
Feed rate (mm/tr)	0.0125	0.025	0.05	0.1
Fz (N)	60	75	90	125
Predicted				
Burr type	Type B or C	Type A	Type A	Type A
bcrit value	0.007	–	–	–
Burr thickness	0.013			
Observation	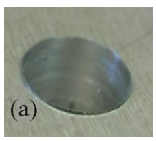 (a)	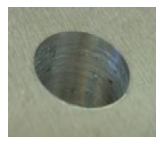	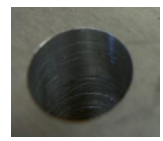	
Measured				
Burr type	Type A	Type A	Type A	Type A
Burr thickness	–	–	–	–

[a] The remaining part of burr has fallen while removing the part from the machine.

3. Experimental verification

3.1. Experimental context

Tests have been conducted on a Huron-K2xl0 cnc machine, and a Kistler multi-component dynamometer 9255B type has been used for force measurements.

A 19.6 mm thick plate of aeronautical aluminum 2024 T354 was set up on to realize experimental validation tests. This ductile material corresponds to the study case of the presented work.

The model is point angle, rake angle and feed rate dependant. So different drills with various geometries have been tested as summarized in Table 1

For all the drills, the clearance angle is 10°. Drills have been especially grinded to obtain the specified rake angle.

For each drill, 5 feed rates have been tested: 0.0125–0.025–0.05–0.1–0.2 mm/tr and each test has been repeated twice. The cutting speed for the main tests is a 60 m/min speed and all the tests are realized in dry machining. Lauderbaugh (2009) detailed that the effect of cutting speed on burr formation is very less important than other parameters and especially than feed rate and cutting angles effects. Nevertheless cutting speed effect is taken into account by its effect on axial cutting force which is used in the model. Verification is done by also doing a 30 m/min and 120 m/min test with drill no. 2.

Specific force measurement tests have been previously conducted with drills mentioned in Table 1 after a 4 mm pre-drilling. This is to evaluate Fz value needed in Eq. (8). Indeed, the loadings to the studied volume (see Fig. 3) have to be evaluated without the effect of the drill web. The tests allowing analyzing burr formation have been conducted without any predrilling. Types B and C of burr thickness have been measured with a micrometer caliper.

3.2. Results and analysis

3.2.1. Burr type and confrontation to the model prediction

For each test, the cutting force is for drilling in a 4 mm predrilled hole. Presented model has been computed by solving Eq. (8) with the solver function of excel software. For each given configuration the bcrit value has been calculated and when this value exists it is mentioned in the table. The value σy, yield strength of workpiece material is set to 324 MPa as detailed by Kalay (2007). Results obtained at 0.2 mm/tr feed rate are not detailed in the following tables since, as with 0.1 mm/tr feed rate, they always present a burr type A

Table 2 presents test results conducted at 60 m/min.

Table 3 presents the results obtained with drill no. 1 at various cutting speed and 0.025 mm/tr feed rate.

3.2.2. Analysis

Burr type prediction. In most cases, model predictions fit the observations in terms of burr type prediction.

Indeed with drill no. 3 at 0.0125 mm/tr feed rate, a B or C burr type was predicted and type A was observed. This point may be explained by

- bcrit value is near zero for this configuration, meaning that this configuration is quite in the transient domain between burr appearance and disappearance;
- a meticulous observation of the hole edge, presented in Fig. 6a, confirms that upper face of the remaining burr presents a breaking pattern showing that this configuration is in a transient domain between burr appearance and disappearance, see for difference Fig. 6b showing hole' edge drilled with the same tool at 0.025 mm/tr feed rate.

The criterion set by the presented model is a binary one: if bcrit value exists, a burr of type B or C should exist. The real cutting is not so binary but analyzing the previous case shows that the transient domain can be determined by the model by studying bcrit value.

Tables 2 and 3 show that distinction between burr type B or C2 cannot be described by this model, and considerations about point angle and cutting speed should be taken in account to explain the phenomenon conducting to a B or C2 burr type. Observed burr types seem coherent since drill no. 4 is more acute than drill no. 2: the

Table 3
Experimental and theoretical results with drill no. at 0.025 mm/tr.

Drill no. 2			
Cutting speed (m/min)	30	60	120
Fz (N)	50	50	40
Predicted			
Burr type	Type B or C	Type B or C	Type B or C
bcrit value	0.013	0.008	0.001
Burr thickness	0.025	0.021	0.013
Observation	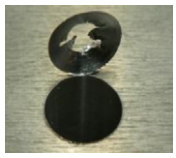		
Measured			
Burr type	Type B	Type B	Type C2
Burr thickness	0.030–0.08	0.029–0.07	0.022

more acute is the drill and the easier it is at splitting the burr cap in a C2 burr.

Burr thickness prediction. Model prediction in terms of thickness fits measurements in case of C2 burr type since predictions and measures are in the same order of magnitude. It is quite different in case of B burr type for which two values are mentioned in Table 2. The highest value corresponds to the thickness measurement at the periphery of the burr cap, the lowest one corresponds to measurement around the middle, where cap is exploded and looks like C2 burr type, see Fig. 7.

Further study could help determining the reason of this thickness variation but a beginning of explanation could be as follows. At the beginning of the burr formation, in the center, the cutting speed is not high enough to let the drill edge passing under the beginning burr, so its thickness is just equal to bcrit + $f/2$ value. But the burr grows at each drill turn and finished to be thicker at the part that is produced at the end of the drill exit, that is at the periphery. At the periphery, cumulated thicknesses due to all previous turns conduce to biggest thickness than in the middle. In the configuration of a burr cap growth, the mechanism should also be different from the studied configuration since cap works more like a membrane or a shell.

4. Conclusion

The experimental verification has shown that the model gives reliable theoretical data regarding burr thickness, and can accurately predict burr type. In comparison with previous works, this study's analytical model considering slip planes theory is based on physical considerations to explain burr formation phenomenon in drilling. Despite a lack of information on precise burr type, the model allows determining cutting conditions and drill geometry in order to get a type 1 of burr which is the one requiring the least removal cost. This kind of approach has already been used in burr prediction in turning by Toropov and Ko (2006), but it was in an orthogonal cutting context with a semi-infinite dimension of the machined part assumption that could not be accepted in drilling. Since the presented model is very different from what have already been developed in drilling, its efficiency can hardly be compared. However, the results concord fully with statements detailed by Lauderbaugh (2009) or Pande and Relekar's (1986) other experimental studies. At very low feed rate, burr eight is the highest and then decreases to its minimum before rising again while feed rate increases. That corresponds to the model prediction since reducing feed rate conduces to bcrit value existence stating a cap appearance prediction, but on the opposite, much increasing feed rate conduces to increase load on remaining part under the drill that produce burr by bending. So there is an optimal feed rate that must be just high enough to avoid burr cap and not too high to avoid thick drilled part bending and conducing to a high burr.

The proposed model can be used in computer manufacturing systems, to predict burr appearance on the edges of drilled parts. The model can also be used in independent burr expert systems so as to minimize burr formation by choosing optimal cutting conditions.

Subsequent studies on burr modeling should focus on the effects of tool wear on burr development as well as the effect of high cutting speed that should modify burr formation phenomenon.

References

Gillespie, L.K., 1975. The $2 billion deburring bill. Manufacturing Engineering Management 74, 20–21.

Heisel, U., Luik, M., Eisseler, R., Schaal, M., 2005. Prediction of parameters for the burr dimensions in short-hole drilling. CIRP Annals: Manufacturing Technology 54 (1), 79–82.

Kachanov, L.M., 1969. Fundamentals of the Theory of Plasticity. Science, Moscow.

Kalay, F., 2007. Simulation numérique de l'usinage – Application à l'aluminium A2024-T351 – Techniques de l'ingénieur.

Khan, I.A., Bhasin, V., Chattopadhyay, J., Ghosh, A.K., 2008. On the equivalence of slip-line fields and work principles for rigid-plastic body in plane strain. International Journal of Solids and Structures 45 (December (25–26)), 6416–6435.

Klocke, F., Hoppe, S., Fritsch, R., 2004. FE-modeling of burr formation in orthogonal cutting. In: Proceedings of the Seventh International Conference on Deburring and Surface Finishing, University of California, Berkeley, 7–9 June 2004, pp. 47–56.

Ko, S.-L., Lee, J.-K., 2001. Analysis of burr formation in drilling with a new-concept drill. Journal of Materials Processing Technology 113 (June (1–3)), 392–398.

Lauderbaugh, K., 2009. Analysis of the effects of process parameters on exit burrs in drilling using a combined simulation and experimental approach. Journal of Materials Processing Technology 209 (February (4)), 1909–1919.

Lauderbaugh, K., Saunders, L., 2003. A finite element model of exit burrs for drilling of metals. Finite Elements in Analysis and Design 40 (December (2)), 139–158.

Lee, E.H., Shaffer, B.W., 1951. The theory of plasticity applied to a problem of machining. Transaction of the ASME 73, 405–413.

Nakayama, K., Arai, M., 1987. Burr formation in metal cutting. Annals of the CIRP 36 (1), 33–36.

Pande, S.S., Relekar, H.P., 1986. Investigations on reducing burr formation in drilling. International Journal of Machine Tool Design and Research 26 (3), 339–348.

Schafer, F., 1978. Gratbildung und Entgraten beim Umfangsstirnfrasen. VDI-Zeitung 120 (1/2), 47–55.

Toropov, A., Ko, S.-L., Kim, B.-K., 2005. Experimental study of burrs formed in feed direction when turning aluminum alloy Al6061-T6. International Journal of Machine Tools and Manufacture 45, 1015–1022.

Toropov, A., Ko S.-L., 2006. A model of burr formation in the feed direction in turning. International Journal of Machine Tools and Manufacture 46 (December (15)), 1913–1920.